Research Article

Yuechao Hui*

Application of improved P-BEM in time varying channel prediction in 5G high-speed mobile communication system

https://doi.org/10.1515/nleng-2024-0085
received October 11, 2024; accepted December 29, 2024

Abstract: To improve people's communication experience on high-speed trains, this study proposed a time-varying channel prediction (TVCP) method based on an improved polynomial basis extension model and backpropagation neural network. The improved polynomial-basis expansion model proposed in this study extracts the optimal basis function by constructing a channel correlation matrix and performing singular value decomposition to adapt to high-speed mobile channel changes. By using these basis functions and pilot signals to estimate historical basis coefficients as training data for back propagation neural network, future channel states can be predicted to improve the accuracy of TVCP in high-speed mobile communication systems. The results showed that when the training sample of the prediction method was 2,000, the maximum mean square error before improvement was close to 0.01, the maximum after improvement was 4.0×10^{-4}. After increasing the normalized Doppler frequency shift to 0.5, the mean square error of the improved method was around 0.0001, while other methods were above 0.001. The improvement of the TVCP method effectively reduced the mean square error of TVCP, the prediction accuracy of the improved prediction method was much superior than that of traditional channel prediction methods. The designed method can greatly perfect the prediction accuracy of time-varying channels and enhance people's communication experience on high-speed trains in high-speed mobile scenarios.

Keywords: 5G communication, communication system, P-BEM, channel prediction

1 Introduction

With the continuous emergence of application scenarios such as the Internet of Things (IoT), intelligent transportation, and virtual reality, people's performance requirements for communication systems are also increasing [1]. The deployment and application of 5G communication systems have become an important reason for promoting the development of digital society. 5G technology can not only achieve faster data transmission rates, but also support the connection of large-scale IoT devices and low latency, high reliability communication services [2,3]. The transmission signal of the communication system may undergo channel changes during the transmission process due to factors such as the movement of the mobile end. Channel changes can continuously alter the state of signal transmission in communication systems, which can have a significant impact on the communication system performance [4,5].

If the channel changes in the transmission signal can be accurately predicted, the signal transmission performance of the communication system can be improved. Xu *et al.* developed a channel extrapolation scheme built on deep learning to reduce pilot overhead and obtain time-varying cascaded channels. The network was segmented into time-domain and antenna-domain extrapolation networks, and differential equations were used. The results showed that this scheme could effectively extrapolate the cascaded reconstruction of intelligent surface channels in high-mobility scenarios [6]. Xu *et al.* designed a three-stage joint channel decomposition and prediction framework to mitigate the effects of shadow fading and obstacle obstruction. This framework utilized the time scale characteristics of the channel, combined with full duplex technology and sparse connection long short-term memory algorithm, to achieve intelligent surface structure capture with low pilot cost and high accuracy [7]. Huang *et al.* put forward a deep learning-based multi-input multi-output radar-assisted millimeter wave channel estimation scheme to improve the robustness in time-varying channels (TVCs),

*** Corresponding author: Yuechao Hui,** School of Mechanical and Electrical Engineering, Suzhou Global Institute, Suzhou, 215163, China, e-mail: hyuechao147@126.com

especially in vehicle for object communication. The design of transmission frame structure for joint radar and communication modules was divided into two stages: arrival/departure and gain estimation. In the face of incomplete array elements, a two-step angle estimation algorithm and a gain estimator based on residual denoising auto-encoder were adopted. Simulation showed that this scheme could efficiently estimate high mobility millimeter wave channels with fewer resources [8]. The application of existing channel prediction and estimation methods in communication systems has certain limitations, mainly manifested in insufficient adaptability to high-speed mobility scenarios, high complexity in processing incomplete array elements, limited prediction accuracy in complex multipath environments, and challenges in computational complexity and resource consumption. Therefore, in order to improve the overall performance of communication systems, new technologies and methods need to be developed to overcome the shortcomings of existing methods, especially in modern communication environments with rapid channel changes and complex and changing channel conditions.

There are various methods for time-varying channel prediction (TVCP), and polynomial-basis expansion model (P-BEM) is one of them. Lefebvre proposed an alternative method using P-BEM and three effective strategies for calculating high-order moments to evaluate the statistical characteristics of the model output while considering the statistical characteristics of uncertain model inputs. This method could support users to make wise choices [9]. Yu *et al.* proposed an uncertainty propagation method grounded on P-BEM to estimate the possibility density and cumulative distribution function of fatigue life of rolling bearings, considering the uncertainty of material parameters. This method could accurately predict the probability fatigue life of rolling bearings under constant and variable loads [10]. Pan *et al.* proposed a sparse solution scheme based on Bayesian regression to overcome the over-fitting and high computational complexity of P-BEM in the estimation of failure probability in geotechnical engineering, combining sequential learning and important sampling techniques. This scheme effectively improved computational efficiency and accurately estimated the probability of small faults using fewer samples [11].

In summary, TVCs with uncertain communication system transmission signals can reflect the signal transmission quality of the communication system. However, the uncertainty, time-varying nature (TVN), diversity, complexity, and dynamism of TVC make TVCP more difficult, and high-speed mobile communication (HSMC) systems further increase the difficulty of predicting TVC in communication systems. In HSMC environments, the acquisition of channel state information (CSI) faces challenges of accuracy, low latency, and low pilot overhead, especially in intelligent surface assisted systems. Due to the large number of passive elements in intelligent surfaces, accurate, low latency, and low pilot overhead CSI acquisition becomes even more difficult. P-BEM is a commonly used method for channel prediction and modeling, which uses polynomial function fitting to capture the nonlinear and TVN of the channel, thereby achieving accurate prediction of TVC. Therefore, to enhance TVCP accuracy in HSMC systems, this study proposes to combine back propagation neural network (BPNN) with P-BEM, and use the combined model to predict TVCP in HSMC systems.

The innovation of the research lies in proposing a TVCP model that combines BPNN and P-BEM. By using P-BEM to obtain the base coefficients of the channel, BPNN is trained for TVCP in HSMC systems. The main contribution of the research is to improve the prediction accuracy of TVC in the HSMC system and improve the signal transmission quality of the HSMC system. This study is conducted from four aspects. Part 1 is a survey of the current research status of TVCP, and Part 2 is a study of TVCP methods combining BPNN and P-BEM. Part 3 is an experimental validation of the constructed method. Part 4 discusses and summarizes the research content of this study.

2 Methods and materials

In this section, this article will provide a detailed introduction to the TVCP method that combines improved P-BEM and BPNN. First, the time-varying characteristics of wireless channels will be analyzed, which is the main reason for the time-varying of channels. This article will explore orthogonal frequency division multiple access (OFDMA) and OFDMA technologies, and how they combat interference and signal fading in communication networks. In addition, the design of pilot structures and how to estimate CSI from pilot symbols will also be discussed. Second, this article will construct an OFDMA communication system model for high-speed mobile scenarios and use P-BEM to model wireless channels. In addition, it is necessary to extract basis functions, estimate the basis coefficients at historical moments, and construct the training dataset for BPNN. Subsequently, the BPNN will be trained and the trained model will be used to predict future time-domain channel coefficients.

2.1 Analysis of TVN of wireless channels in HSMC systems

The TVNs of wireless channels are the main cause of channel variability. Orthogonal frequency technology is a

technique that can combat interference and signal fading in communication networks, but its application range is limited due to the low efficiency of spectrum resource utilization [12,13]. OFDMA is a multi-access technology proposed by combining orthogonal frequency technology and frequency division multiplexing technology. This technology divides the signal transmission bandwidth into multiple orthogonal subcarrier sets and allocates resources according to user needs, making it the current mainstream multiple access solution. The structure of the transmitting and receiving ends of this scheme is shown in Figure 1 [5,14].

At the transmitting end, communication participants are assigned to different sub-carriers, and then adaptive modulators are selected based on user needs to select the pairing method with the highest compatibility between sub-carriers and user channel conditions. The matched sub-carriers are first subjected to high-order modulation, and then, consistent with traditional orthogonal frequency techniques, the signal is transmitted. The operation of the receiving end and the transmitting end is opposite. Channel prediction is the process of predicting future states through the historical state of a channel during signal transmission. The core content of channel prediction is the acquisition of historical states, which rely on the CSI

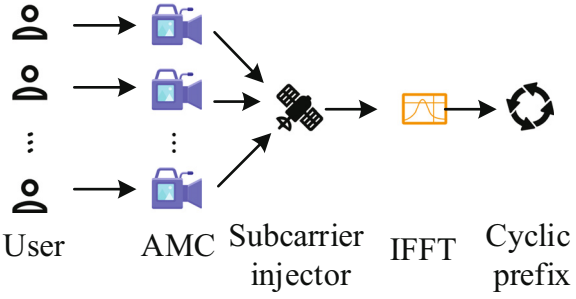

Figure 1: OFDMA structure.

estimated by pilot symbols. The pilot symbols of different pilot structures are different, and channel prediction is directly related to the number and position of pilots. Pilot structures can reflect the number and position of pilots. The pilot structure includes comb shaped pilots inserted at intermediate intervals in the frequency domain, block-shaped structures distributed at intermediate intervals in the time domain, and lattice structures inserted at intermediate intervals in the time and frequency domains, as shown in Figure 2 [15,16].

In a comb-shaped pilot structure, the pilot is continuously distributed in the time domain. In a block like structure, pilots are continuously distributed in the frequency domain. The pilot in the lattice structure is discontinuous in both domains. In comb-like structures, signals have strong resistance to time selective fading and have better performance in HSMC scenarios [17,18].

In block like structures, signals have strong resistance to frequency selective fading. When obtaining signal state information in HSMC scenarios, this structure requires more pilots, which can increase computational complexity and reduce system efficiency. The lattice structure has weak resistance to signal fading, but when obtaining historical CSI using this structure, intelligent algorithms can be used to calculate the position of data symbols, improving the performance of communication systems. The TVNs of wireless channels include multi-path effects and Doppler frequency shift (DFS) effects, as shown in Figure 3.

Multi-path effect refers to the change in the transmission path of electromagnetic waves caused by the reflection or refraction of signals in contact with obstacles during transmission, resulting in the signal received by the terminal being a multi-path superimposed signal. After the superposition of signal paths, the amplitude and phase of the signal change, resulting in channel

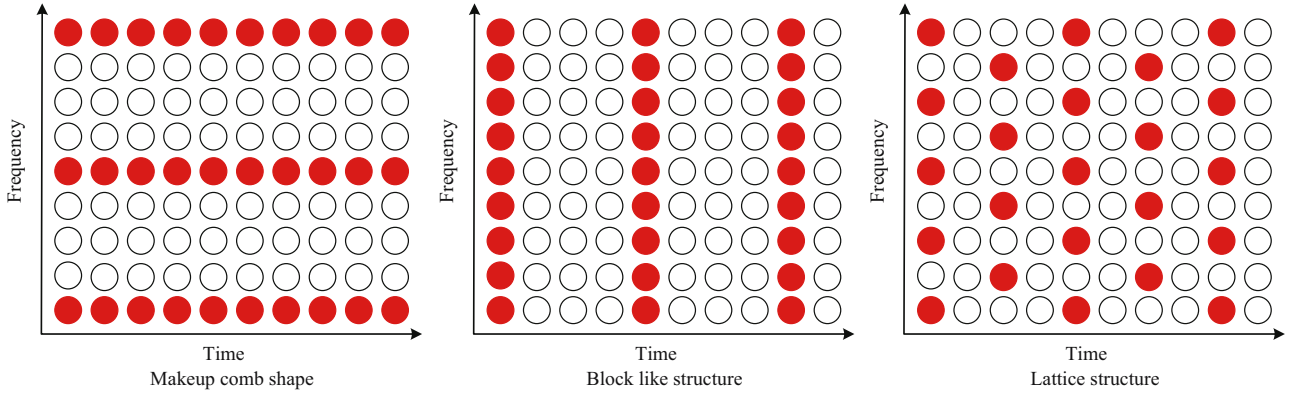

Figure 2: Pilot structure design.

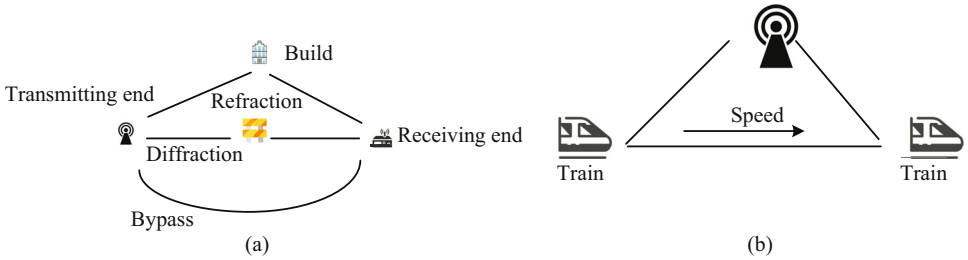

Figure 3: Multi-path effect and the DFS effect. (a) Multipath effect. (b) Frequency shift benefits.

attenuation. The DFS effect is a phenomenon where the phase and frequency alter because of the difference in propagation distance when the wave source moves in a certain direction at a constant rate. The DFS can be calculated using Eq. (1).

$$f_d = \frac{v}{\lambda}\cos\theta = \frac{vf_c}{c}\cos\theta, \tag{1}$$

where f_d represents DFS. v represents the relative movement speed between the transmitting end and the receiving end. c is the light speed. f_c denotes the carrier frequency. θ represents the angle between the direction of movement of the transmitting end and the receiving end. In high-speed mobile scenarios, the DFS effect is the main cause of channel changes. The communication scenario during high-speed rail operation is the most common HSMC scenario in daily life. The wireless communication channel (WCC) model in this scenario is the Rice channel of the scenic spot. The signals of this type of channel has two types: sight line and non-line of sight propagation. The latter component is a constant with Doppler frequency offset, which is complex fading under the influence of Doppler. In communication systems, the channel representation for transmitting signals is given in Eq. (2).

$$\begin{aligned} h_i(m,n) = {} & c_i \exp[j2\pi\varepsilon_{i,m}(mN_S - N + n)/N] \\ & + \sum_{l_p=0}^{L-1} a_{i,l_p}(m,n)\delta(m, n - \tau_{l_p}), \end{aligned} \tag{2}$$

where i represents the signal transmission sub-frame index. m represents the symbol index on the sub-frame. n represents the channel sampling point index. c_i represents the line-of-sight propagation component of the channel. $\varepsilon_{i,m}$ represents normalized Doppler frequency offset. N represents the length of Fourier transform and inverse Fourier transform. L is the number of channel paths. τ_{l_p} is the normalized delay of the l_pth path. N_S represents the sum of the loop length and N. δ represents a constant. $a_{i,l_p}(m,n)$ represents the scattering path. The normalized Doppler frequency offset can be calculated using Eq. (3).

$$\varepsilon_{i,m} = f_d/\Delta f, \tag{3}$$

where f_d represents the DFS between the transmitter and receiver in the communication system. Δf represents the sub-carrier spacing. There are two different expressions for the Rice factor of the Rice channel. The first one represents the entire channel, as shown in Eq. (4).

$$k = |c_i|^2/P_s, \tag{4}$$

where k represents the Rice factor. P_s represents the sum of the covariance of the scattering components. The second method is the ratio of the line-of-sight propagation component to the non-line-of-sight propagation component on the first path, as shown in Eq. (5).

$$k = |c_i|^2/\mathrm{var}[a_{i,0}], \tag{5}$$

where var[·] represents the covariance of the scattering component. var$[a_{i,0}]$ represents the component of non-line-of-sight propagation on the first path.

2.2 TVCP combining P-BEM and BPNN

In HSMC systems, the prediction of TVCs faces the complexity of rapid signal changes and multipath effects. Although the traditional P-BEM method can capture the nonlinear and time-varying characteristics of the channel through polynomial function fitting, its fixed basis function may not accurately reflect the dynamic changes of the channel in high-speed moving environments. The advantage of P-BEM lies in its ability to use polynomial functions to fit and capture the nonlinear and time-varying characteristics of the channel. However, traditional P-BEM has limited predictive ability when facing rapid channel changes in high-speed mobile environments. BPNN can learn and extract the characteristics of channel changes from a large amount of historical data, which can be used as parameters for polynomial fitting in P-BEM, enabling the basic function of P-BEM to dynamically adapt to channel changes. Therefore, the study proposes to

combine P-BEM with BPNN to improve the accuracy of TVCP. This model includes receiving antennas N_r and transmitting antennas N_t, and different antenna pilots need to maintain orthogonality. The pilot structure is a comb like structure. The oth symbol received by the system receiver is given by Eq. (6).

$$R_o = H_o S_o + W_o, \tag{6}$$

where o represents the symbol index. R represents the symbol received by the receiving end. S represents the symbol of the transmitting end. W represents a Gaussian white noise vector. H represents the frequency domain channel matrix. The expression of H is given by Eq. (7).

$$H_o = \begin{bmatrix} H_o^{(1,1)} & \cdots & H_o^{(1,t)} & \cdots & H_o^{(1,N_t)} \\ \vdots & \ddots & \vdots & \ddots & \vdots \\ H_o^{(r,1)} & \cdots & H_o^{(r,t)} & \cdots & H_o^{(r,N_t)} \\ \vdots & \ddots & \vdots & \ddots & \vdots \\ H_o^{(N_r,1)} & \cdots & H_o^{(N_r,t)} & \cdots & H_o^{(N_r,N_t)} \end{bmatrix}. \tag{7}$$

The $[H_o^{(r,t)}]$ in Eq. (7) can be calculated using Eq. (8).

$$[H_o^{(r,t)}] = \frac{1}{N}\sum_{l=0}^{L-1} e^{\frac{-j2\pi i' l}{N}} \sum_{n=0}^{N-1} h_{l,o}^{(r,t)}(n) e^{\frac{-j2\pi(i'-i)n}{N}}, \tag{8}$$

where h represents the sampling point channel, and r is the receiving antenna index. t represents the index of the transmitting antenna. l represents the path index. BEM can simulate wireless channels using basis functions. Therefore, when conducting prediction research on WCCs, BEM is used to model the wireless channels. The solution based on the BEM principle is calculated using Eq. (9) [19,20].

$$h_{l,o}^{(r,t)}(n) = \sum b_{p,q} c_{q,l,o}^{(r,t)} + \varepsilon_{l,o}^{(r,t)}(n), \tag{9}$$

where $b_{p,q}$ represents the qth element of the pth basis function. c represents the basis coefficient corresponding to the basis function. ε represents the error in channel modeling by BEM. When modeling wireless channels using BEM, the frequency domain channel matrix $\mathbf{H}_o^{r,t}$ can be expressed using Eq. (10).

$$\mathbf{H}_o^{r,t} = \sum_{q=0}^{Q-1} \mathbf{M}_q \mathrm{diag}\{\mathbf{F}\mathbf{c}_{q,o}^{r,t}\}, \tag{10}$$

where diag{·} is the operation of converting a vector into a diagonal matrix. $\mathbf{M}_q$ represents a matrix of $N \times N$ dimensions. $\mathbf{F}$ represents the Fourier transform matrix. $\mathbf{c}$ is the basis coefficient vector. The method of using P-BEM combined with BPNN for TVCP is to model the channel using P-BEM, and then calculate the estimated base coefficients of the past channel based on the received signal at the pilot using the least squares method. Using the estimated value of the base coefficient to construct the base coefficient sample as the training data of BPNN. Finally, using the estimated values of the past base coefficients of the channel as input for the trained prediction model, the future time-domain channel coefficients are predicted. The specific process can be divided into three steps. First, the historical basis coefficients for wireless channels based on P-BEM are estimated. Second is the training of neural networks. Finally, the wireless channel information are predicted. Traditional P-BEM is fixed in practical applications and cannot reflect the changing wireless channels in high-speed mobility. This study proposes to improve P-BEM and optimize its channel modeling [21,22]. The improvement of P-BEM is mainly reflected in the acquisition of wireless channel matrix. The improved P-BEM constructs a channel correlation matrix based on past channel information, and then extracts basis functions from the channel correlation matrix to model the wireless channel. In the improved P-BEM, assume that the ideal frequency domain channel information at time t is $\mathbf{H}_o$ and the channel correlation matrix is $\mathbf{P}_o$, to perform singular value decomposition $\mathbf{P}_o$, as shown in Eq. (11).

$$\mathbf{P}_o = \mathbf{J}_o \wedge_o \vee_o , \tag{11}$$

where $\wedge_o$ represents a diagonal matrix composed of the eigenvalues of $\mathbf{P}_o$ in descending order. $\mathbf{J}_o$ represents the eigenvector matrix. At this point, the optimal basis function matrix $\mathbf{B}_o$ is the first Q column of $\mathbf{J}_o$. Using $\mathbf{B}_o$, the wireless channel is modeled and the base coefficients are estimated, as shown in Eq. (12).

$$\hat{\mathbf{c}}_o = (\tilde{\Gamma}_o^H \tilde{\Gamma}_o)^{-1} \tilde{\Gamma}_o^H \tilde{\mathbf{R}}_o, \tag{12}$$

where $\tilde{\mathbf{R}}_o$ represents the pilot signal received on the frequency domain OFDMA symbol. $\tilde{\Gamma}_o$ represents the submatrix of Γ_o at the pilot position. After obtaining the basis coefficients based on the optimal basis function matrix $\mathbf{B}_o$, the training of BPNN can begin. When training BPNN, it is necessary to obtain the estimated base coefficients of past

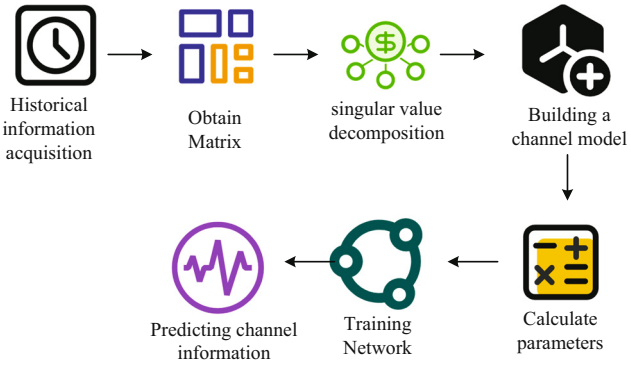

Figure 4: Improvement of the TVCP process of P-BEM with BPNN.

moments according to Eq. (12) and construct a training sample set, as calculated using Eq. (13).

$$\Omega = \{(X^{(1)}, Y^{(1)}), \cdots, (X^{(U)}, Y^{(U)})\}, \tag{13}$$

where U means the quantity of training samples. $X^{(1)}$ denotes the input sample constructed by past base coefficient estimation. $Y^{(1)}$ represents the output sample. After constructing the training set, the BPNN can be trained using the conventional training method. After completing the training, the estimated base coefficients of any of the first G moments in the WCC are used as inputs for predicting the future channel. Figure 4 shows the TVCP process of the HSMC system constructed by combining improved P-BEM and BPNN.

The steps to predict the WCC of the HSMC system are as follows: Step 1 is to obtain the channel correlation matrix based on the historical information of WCC. Step 2 is to perform singular value decomposition on the channel correlation matrix to obtain the optimal basis function for P-BEM. Step 3 is to model WCC using P-BEM based on the optimal basis function. Step 4 is to use the pilot signals received in the past and the optimal basis function to calculate the estimated base coefficients at historical times. Step 5 is to calculate the ideal channel basis coefficient at time t. Step 6 is to construct a training dataset for BPNN based on the estimated base coefficients and ideal base coefficients. Step 7 is to set the training parameters for BPNN and train it. Step 8 is to input the estimated base coefficients from any of the first G moments and predict the CSI for future moments.

3 Results

3.1 Experimental environment and parameter settings

A TVCP method for HSMC systems based on P-BEM and BPNN was studied and improved. To verify the feasibility of the designed channel prediction method (CPM) and its improvements, a simulation experimental environment was established. Simulation tests were conducted on the improved and unimproved CPMs. The experimental operating system is Windows 10 Professional, with Intel Core i9-10900K CPU, NVIDIA GeForce RTX 3080 GPU, and 32.0GB system memory. In the HSMC system, the symbol length, cyclic prefix length, carrier frequency, sub-carrier spacing, train speed, channel model, and number of basic functions of the transmitting antenna, receiving antenna, and OFDMA are important parameters. The number of hidden layer neurons, training error, and maximum number of iterations are important parameters of BPNN. Wang *et al.* and Ma *et al.* conducted research and analysis on TVCP schemes in different network environments, and achieved certain results. Therefore, the study referred to the relevant research of these scholars to design simulation test network parameters, as shown in Tables 1 and 2 [23,24].

In the BPNN model, the study selected 5 hidden layer neurons (improved) and 20 hidden layer neurons (pre improved) to balance the model's learning ability and computational efficiency. Fewer neurons reduce model complexity and training time, while an appropriate number of neurons ensure the ability to capture channel changes. The maximum number of iterations and training error are set based on the model convergence speed and prediction accuracy, respectively, from 3,000 to 1,000 iterations, and from 1,000 to 3,000 iterations to achieve finer training stopping conditions. The sample size has been increased from 100 to 2,000 in order to improve the model's generalization ability and prediction accuracy, especially in high-speed moving scenarios where the effect is significant. These choices take into account data diversity, training efficiency, and prediction accuracy. This study compared the performance of two improved CPMs from five aspects during simulation testing. The first method is the mean squared error (MSE) of two methods at different training sample sizes. The second type is the training time at different numbers of training samples. The third type is MSE with different training methods. The fourth type is MSE for different prediction methods, and the fifth type is analysis of computational complexity.

Table 1: Communication system parameter settings

Name	Value	Name	Value
Sending antenna	2	Receiving antenna	2
Symbol length for OFDMA	128	Loop prefix length	16
Carrier frequency	2.35 GHz	Sub-carrier spacing	15 kHz
Train speed	500 km/h	Channel model	5-channel Rice channel
Rice factor	5	Number of basic functions	4

Table 2: BPNN parameter settings

Name	Before improvement Value	After improvement Value
Number of hidden layer neurons	20	5
Maximum number of iterations	3,000	1,000
Training error	10^{-4}	10^{-4}

3.2 Analysis of channel prediction simulation results

The training samples have a significant impact on the training effectiveness of the model. This study compared the MSE of the two improved CPMs before and after the improvement under different training sample numbers, as shown in Figure 5.

Figure 5(a) shows the MSE of the pre-improved prediction scheme under different training samples. When the signal-to-noise ratio (SNR) was the same, the higher the training samples, the lower the MSE of the model. When the training samples were 100 and 2,000, the maximum MSE was close to 1 and 0.01. As the training data increased, the prediction accuracy would also gradually increase. Figure 5(b) shows the MSE of the improved prediction scheme under different training samples. The impact of training samples on the improved CPM was consistent with the original scheme, and the model MSE increased with the increase in training samples. Table 3 shows the training time of the two CPMs before and after improvement under different training sample sizes.

In Table 3, the pre-improved CPM significantly increased training time as the number of training samples increased. When the training sample increased from 100 to 2,000, the training time increased from about 10 s to over 780 s. After improvement, the training time of the CPM would also increase with the rise of the training samples, but the rise speed would significantly decrease. When the training sample increased from 100 to 2,000, the training time increased from about 2 s to about 30 s. Figure 6 shows the impact of different training methods on channel prediction performance.

Table 3: Effect of the number of training samples on the time-consuming cost of the model training

Before improvement		After improvement	
Sample size	Time (s)	Sample size	Time (s)
100	9.22	100	2.30
500	143.81	500	8.68
1,000	466.71	1,000	16.63
2,000	787.44	2,000	30.69

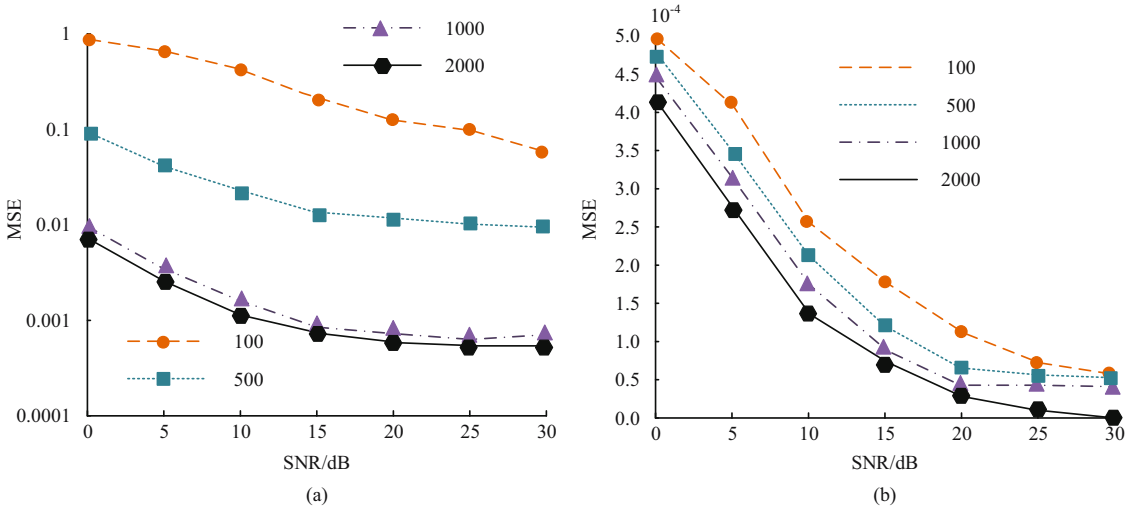

Figure 5: Effect of the training samples on the model training. (a) The impact of sample size on the pre-improved CPM. (b) The impact of sample size on improved CPMs.

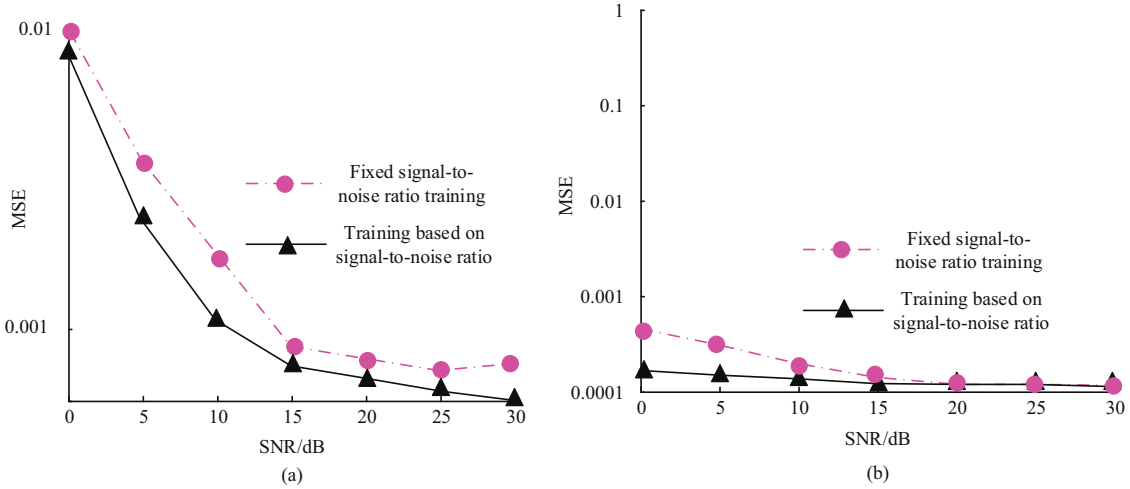

Figure 6: Effect of different training methods on the channel prediction performance. (a) The impact of sample size on the pre-improved CPM. (b) The impact of sample size on improved CPMs.

Figure 6(a) and (b) shows the impact of different training methods on the pre-improved and improved CPM. In Figure 6(a), when training with fixed SNR and training-based SNR, the MSE of the CPM was highest at around 0.01 and 0.009. The training-based SNR was slightly lower than the fixed SNR training method, and as the SNR increased, the difference between the two would also become larger. In Figure 6(b), as the SNR increased, the MSE of the two training methods gradually tended to be consistent. When the SNR was low, the MSE value of the training-based SNR method was smaller. To further analyze the feasibility of the proposed CPM, the improving path channel estimation (IPCE) in the research by Li and Mitra [21] and the membership filtering (MF) in the research by Zhao *et al.* [22] were compared with the research method. Meanwhile, this article also compared it with the dual channel transferable RUL model proposed by Guo *et al.* [25]. Figure 7 shows the comparison results of MES performance under normalized DFS using different prediction methods.

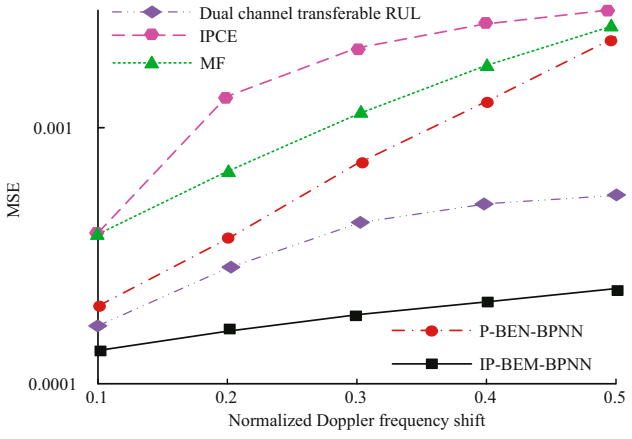

Figure 7: Change in the channel prediction performance with the normalized DFS.

In Figure 7, as the normalized DFS increased, the MSE of all methods increased. When the normalized DFS was 0.1, the MSE of all methods was below 0.001. After increasing the normalized DFS to 0.5, the MSE of the improved method was around 0.0001, while the MSE of other methods was above 0.001. As the Doppler shift continues to increase, the MSE values of different methods also increase slightly, but it can still be observed that the MSE value of the improved P-BEM model designed in the study remains at a low level. This indicates that the model designed for research is recognized to maintain good basic performance under the continuous increase of DFS. The normalized DFS had the least interference on the designed CPM, and the improved CPM performed the best in HSMS. The analysis of complexity was calculated. The complexity of historical information obtained, model training complexity, and prediction complexity were expanded into three dimensions.

Figure 8 shows the complexity comparison of obtaining historical information. In Figure 8(a), the complexity of the historical information obtained by the research method was much higher than that of the methods in the research by Li and Mitra [21] and Zhao *et al.* [22]. As the number of sub-carriers increased, the complexity of obtaining historical information would gradually increase. The changes in Figure 8(b) are consistent with Figure 8(a). Figure 9 shows a comparison of model training complexity.

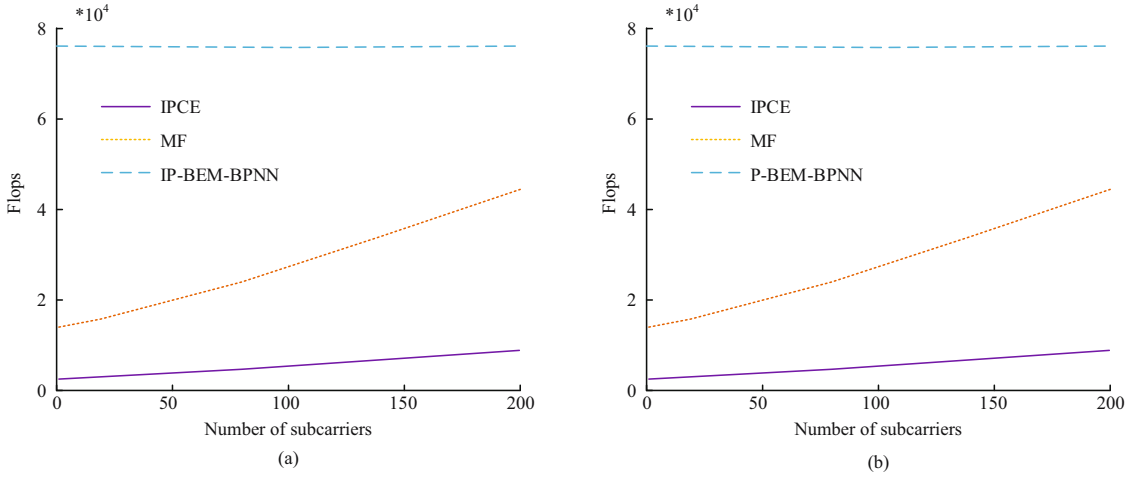

Figure 8: Comparison of the complexity of obtaining historical information. (a) After improvement. (b) Before improvement.

Figure 9 showed the comparison of training complexity between MF and the improved and pre-improved P-BEM-BPNN methods. In Figure 9(a), the training complexity of the P-BEM-BPNN method did not increase with the increase in the quantity of sub-carriers, which is always below 1×10^{-7}, while the training complexity of MF would continue to increase with the increase in the number of sub-carriers. In Figure 9(b), the training complexity of both methods increased with the increase in the number of sub-carriers. When the number of sub-carriers was higher than 20, the training complexity of the P-BEM-BPNN method was lower. Figure 10 shows a comparison of model prediction complexity.

Figure 10 showed the comparison of prediction complexity between IPCE, MF, and P-BEM-BPNN methods before and after improvement. In Figure 10(a), the IPCE method had the lowest prediction complexity, followed by the improved P-BEM-BPNN method. The prediction complexity of these two methods did not increase with the number of sub-carriers. In Figure 10(b), the prediction complexity of the IPCE method was basically 0, while the prediction complexity of the other two methods increased with the number of sub-carriers.

The study further compared the prediction complexity of three models, IPCE, MF, and IP-BEM-BPNN, with the variation in device computing resources. The results are shown in Figure 11. Figure 11(a) shows the change in model prediction complexity with the increase in device computing resources before model optimization. As can be seen, with the continuous increase in device computing resources, the complexity of model prediction will gradually decrease. Figure 11(a) shows that after model

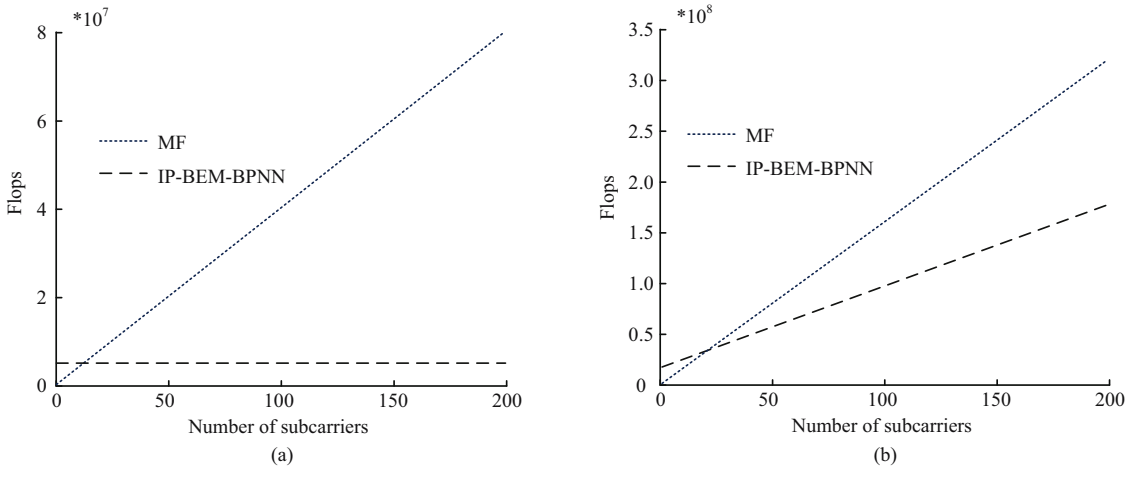

Figure 9: Training complexity comparison. (a) After improvement. (b) Before improvement.

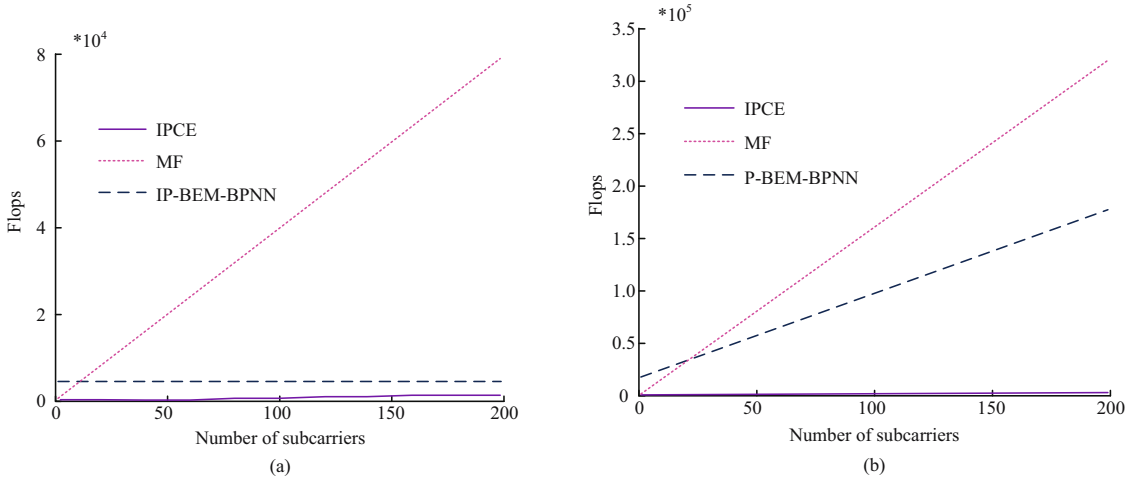

Figure 10: Predictive complexity comparison results. (a) After improvement. (b) Before improvement.

optimization, with the continuous increase in device computing resources, the prediction complexity of the IP-BEM-BPNN model remains basically unchanged and at a lower level.

4 Discussion

The improved time-varying CPM proposed in this article has achieved significant results in HSMC systems. First, regarding the improvement of training time, when the number of training samples increased from 100 to 2,000, the training time of the improved CPM model increased from about 10 s to about 30 s, while the training time of the original model increased from about 10 s to over 780 s. This significant reduction in training time means that our model has significantly improved training efficiency while maintaining prediction accuracy. Compared with the improved atomic norm based time-varying multipath channel estimation method proposed by Li and Mitra [21], the training time significantly increases with the increase in sample size. The improved CPM model proposed in this study has a significant advantage in training efficiency. This improvement is particularly important for HSMC systems that require rapid deployment and real-time model updates, as it reduces the system's waiting time for channel prediction model updates. Second, the improved CPM model studied maintains an MSE of around 0.0001 when the normalized Doppler shift is increased to 0.5, while the MSE of other methods is above 0.001. The decrease in MSE represents a significant improvement in prediction accuracy. According to Lefebvre's (2020) research [10], the P-BEM method proposed by him has an

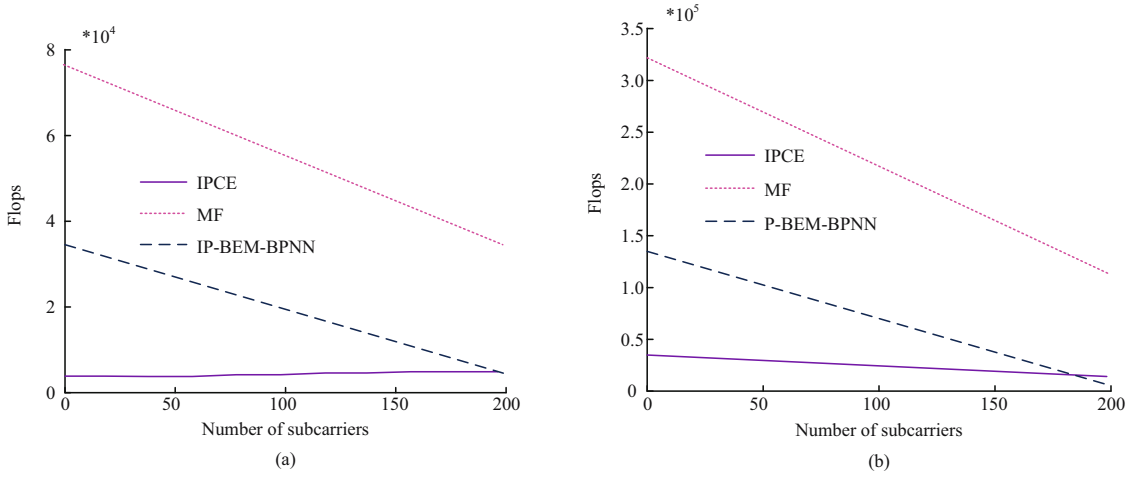

Figure 11: Prediction complexity changes with device computing resources. (a) After improvement. (b) Before improvement.

MSE value close to 0.001 when evaluating the statistical characteristics of the model output. Compared to this, the MSE value of the improved CPM model in this article is lower, indicating a significant improvement in prediction accuracy. A low MSE value means that the difference between the predicted channel state and the actual channel state is smaller, which is crucial for the design and optimization of communication systems as it directly affects the transmission quality of signals and the reliability of the system [26,27]. In addition, the reduction in MSE also means that our model is more effective in dealing with complex channel changes in high-speed mobile scenarios. In these scenarios, the rapid changes in channels place higher demands on prediction models. The model in this article provides more accurate prediction results by dynamically adapting to channel changes, which is of great significance for improving communication quality in mobile environments such as high-speed trains.

The model of this study is based on the combination of P-BEM and BPNN, which assume that channel changes can be effectively predicted through historical data. However, this assumption may not apply to all channel environments, especially in the presence of extreme interference or atypical channel conditions. The performance of the model may be affected by the complexity of channel changes, such as in highly dynamic urban environments where rapid changes in buildings and other obstacles can lead to inaccurate model predictions. Although the model performs well under laboratory conditions, it may face scalability issues in practical deployment. As the scale of the network expands and the number of users increases, the model may require more computing resources to maintain prediction accuracy. In a multi-user environment, the model needs to process more data and more complex CSI, which may lead to an increase in computational complexity and energy consumption, limiting the application of the model on resource constrained devices.

In summary, the improved CPM model proposed in this article not only demonstrates its superiority in theory, but also has significant advantages in practical applications.

5 Conclusion

The TVCP method proposed in this article, which combines the improved P-BEM with BPNN, has important practical application significance in 5G HSMC systems. The key achievements are summarized as follows: First, by constructing channel correlation matrices and performing singular value decomposition, the optimal basis functions were extracted, effectively adapting to the changes in high-speed mobile channels. Second, using these basis functions and pilot signals to estimate historical basis coefficients as training data for BPNN, accurate prediction of future channel states has been achieved. The experimental results show that the improved method reduces the maximum MSE from nearly 0.01 to 4.0×10^{-4} when the training samples are 2,000. After increasing the normalized Doppler shift to 0.5, the MSE remains at around 0.0001, far lower than other methods, demonstrating excellent predictive performance.

In terms of potential applications, the method proposed in this article can significantly enhance the communication experience in high-speed mobile scenarios such as high-speed trains, improve signal transmission quality, and is of great significance for improving the performance of 5G and future 6G communication systems. In addition, this method also has broad application prospects in high-speed data transmission in fields such as intelligent transportation, telemedicine, and virtual reality.

Future research can further optimize algorithms based on this, reduce computational complexity, improve real-time performance, and make them more suitable for practical HSMC systems. Meanwhile, it can be considered to apply this method to a wider range of channel environments and different communication standards to verify its generalization ability and robustness. In addition, combining the latest artificial intelligence technologies such as deep learning and machine learning to further explore and improve the accuracy and efficiency of TVCP is also a direction worthy of in-depth research.

Funding information: Author states no funding involved.

Author contribution: The author has accepted responsibility for the entire content of this manuscript and approved its submission.

Conflict of interest: The author states no conflict of interest.

Data availability statement: All data generated or analyzed during this study are included in this published article.

References

[1] Wang CX, Huang J, Wang H, Gao X, You X, Hao Y. 6G wireless channel measurements and models: Trends and challenges. IEEE Veh Technol Mag. 2020;15(4):22–32.

[2] Li S, Lin S, Cai L, Li W, Zhu G. Joint resource allocation and computation offloading with time-varying fading channel in vehicular edge computing. IEEE Trans Veh Technol. 2020;69(3):3384–98.
[3] Tang W, Chen MZ, Dai JY, Zeng Y, Zhao X, Cui TJ, et al. Wireless communications with programmable metasurface: New paradigms, opportunities, and challenges on transceiver design. IEEE Wirel Commun. 2020;27(2):180–7.
[4] Chowdhury MZ, Hasan MK, Shahjalal M, Hossan MT, Jang YM. Optical wireless hybrid networks: Trends, opportunities, challenges, and research directions. IEEE Commun Surv Tutor. 2020;22(2):930–66.
[5] Yang L, Meng F, Zhang J, Hasna MO, Di Renzo M. On the performance of RIS-assisted dual-hop UAV communication systems. IEEE Trans Veh Technol. 2020;69(9):10385–90.
[6] Xu M, Zhang S, Ma J, Dobre OA. Deep learning-based time-varying channel estimation for RIS assisted communication. IEEE Commun Lett. 2021;26(1):94–8.
[7] Xu W, An J, Xu Y, Huang C, Gan L, Yuen C. Time-varying channel prediction for RIS-assisted MU-MISO networks via deep learning. IEEE Trans Cognit Commun Netw. 2022;8(4):1802–15.
[8] Huang S, Zhang M, Gao Y, Feng Z. MIMO radar aided mmWave time-varying channel estimation in MU-MIMO V2X communications. IEEE Trans Wirel Commun. 2021;20(11):7581–94.
[9] Tang H, Wang J, Song L, Song J. Minimizing age of information with power constraints: Multi-user opportunistic scheduling in multi-state time-varying channels. IEEE J Sel Areas Commun. 2020;38(5):854–68.
[10] Lefebvre T. On moment estimation from polynomial chaos expansion models. IEEE Control Syst Lett. 2020;5(5):1519–24.
[11] Yu A, Li YF, Huang HZ, Tong H, Diao Q. Probabilistic fatigue life prediction of bearings via the generalized polynomial chaos expansion. J Mech Sci Technol. 2022;36(10):4885–94.
[12] Pan Q, Qu X, Liu L, Dias D. A sequential sparse polynomial chaos expansion using Bayesian regression for geotechnical reliability estimations. Int J Numer Anal Methods Geomech. 2020;44(6):874–89.
[13] Liu X, Sun Q. Damage mechanics based probabilistic high-cycle fatigue life prediction for Al 2024-T3 using non-intrusive polynomial chaos. Fatigue Fract Eng Mater Struct. 2020;43(8):1814–23.
[14] Yang L, Yang J, Xie W, Hasna MO, Tsiftsis T, Di Renzo M. Secrecy performance analysis of RIS-aided wireless communication systems. IEEE Trans Veh Technol. 2020;69(10):12296–300.
[15] Cao H, Wu Y, Bao Y, Feng X, Wan S, Qian C. UTrans-Net: A model for short-term precipitation prediction. Artif Intell Appl. 2023;1(2):106–13.
[16] Hu C, Dai L, Han S, Wang X. Two-timescale channel estimation for reconfigurable intelligent surface aided wireless communications. IEEE Trans Commun. 2021;69(11):7736–47.
[17] Zhou G, Pan C, Ren H, Wang K, Di Renzo M, Nallanathan A. Robust beamforming design for intelligent reflecting surface aided MISO communication systems. IEEE Wirel Commun Lett. 2020;9(10):1658–62.
[18] Stergiou CL, Psannis KE, Gupta BB. IoT-based big data secure management in the fog over a 6G wireless network. IEEE Internet Things J. 2020;8(7):5164–71.
[19] Zheng B, You C, Mei W, Zhang R. A survey on channel estimation and practical passive beamforming design for intelligent reflecting surface aided wireless communications. IEEE Commun Surv Tutor. 2022;24(2):1035–71.
[20] Wang CX, Di Renzo M, Stanczak S, Wang S, Larsson EG. Artificial intelligence enabled wireless networking for 5G and beyond: Recent advances and future challenges. IEEE Wirel Commun. 2020;27(1):16–23.
[21] Li J, Mitra U. Improved atomic norm based time-varying multipath channel estimation. IEEE Trans Commun. 2021;69(9):6225–35.
[22] Zhao Z, Wang Z, Zou L, Guo J. Set-membership filtering for time-varying complex networks with uniform quantisations over randomly delayed redundant channels. Int J Syst Sci. 2020;51(16):3364–77.
[23] Wang S, Yao R, Tsiftsis TA, Miridakis NI, Qi N. Signal detection in uplink time-varying OFDM systems using RNN with bidirectional LSTM. IEEE Wirel Commun Lett. 2020;9(11):1947–51.
[24] Ma J, Zhang S, Li H, Gao F, Han Z. Time-varying downlink channel tracking for quantized massive MIMO networks. IEEE Trans Wirel Commun. 2020;19(10):6721–36.
[25] Guo J, Wang Z, Yang Y, Song Y, Wan JL, Huang CG. A dual-channel transferable RUL prediction method integrated with Bayesian deep learning and domain adaptation for rolling bearings. Qual Reliab Eng Int. 2024;40(5):2348–66.
[26] Kouka N, Fourati R, Baghdadi A, Siarry P, Adel M. A mutual information-based many-objective optimization method for EEG channel selection in the epileptic seizure prediction task. Cogn Comput. 2024;16(3):1268–86.
[27] Huang Y, Wang H, Yin H, Zhao Z. Iterative time-varying channel prediction based on the vector Prony method. Wirel Pers Commun. 2024;136(1):103–22.